Macromolecular Research, Vol. 16, No. 6, pp 492-502 (2008)

Cutting Fluid Effluent Removal by Adsorption on Chitosan and SDS-Modified Chitosan

Kowit Piyamongkala, Lursuang Mekasut, and Sangobtip Pongstabodee*

Department of Chemical Technology, Faculty of Science, Chulalongkorn University, Bangkok, 10330, Thailand

Received July 11, 2007; Revised April 11, 2008; Accepted April 11, 2008

Abstract: This study examined the adsorption of a synthetic cutting fluid and cutting fluid effluent on chitosan and SDS-modified chitosan. Chitosan and SDS-modified chitosan were prepared in form of beads and fibers. A series of batch experiments were carried out as a function of the initial concentration of cutting fluid, contact time and pH of the fluid. The contact angle study suggested that the SDS-modified chitosan was more hydrophobic than chitosan. The Zeta potential study showed that chitosan, SDS-modified chitosan and synthetic cutting fluid had a point of zero charge (PZC) at pH 7.8, 9 and 3.2, respectively. SDS-modified chitosan has a greater adsorption capacity than chitosan. The experimental results show that adsorption capacity of the cutting fluid on 1.0 g of SDS-modified chitosan at pH 3 and for a contact time of 120 min was approximately 2,500 g/kg. The adsorption capacity of chitosan and SDS-modified chitosan increased with decreasing pH. The Langmuir, Freundlich, and Brunauer Emmett and Teller (BET) adsorption models were used to explain the adsorption isotherm. The Langmuir isotherm fitted well with the experimental data of chitosan while the BET isotherm fitted well with the SDS-modified chitosan data. Pseudo first- and second-order kinetic models and intraparticle diffusion model were used to examine the kinetic data. The experimental data was fitted well to a pseudo second-order kinetic model. The significant uptake of cutting fluid on chitosan and SDS-modified chitosan were demonstrated by FT-IR spectroscopy, SEM and heat of combustion.

Keywords: cutting fluid, adsorption isotherm, adsorption rate, chitosan, SDS-modified chitosan.

Introduction

Cutting fluid is used in the production process elements of machining operation included turning, drilling, grinding and milling. It plays a significant role in extending tool life and shaping quality of work. The primary function of cutting fluid is to provide lubrication and to dissipate heat between the face of the tool and the metal being cut. The secondary function is to flush fin-chips from tool and work-piece interface in order to prevent the incident of built-up edge. The type of cutting fluid used for machining operations is oil-based and water-based. The oil-based, called straight oil, consists of natural oil and synthetic oil. The natural oil is obtained from animal, marine and vegetable oil, while the synthetic oil is refined mineral oil. The water-based, devided to soluble oil; synthetic and semisynthetic, is mixed by water to form oil-in-water emulsion. Material used as a lubrication matter in soluble oil, synthetic and semisynthetic cutting fluid is mineral oil, organic compounds of polyalphaolefins and the mixture of mineral oil and organic compounds, respectively. Typical additives in the water-based cutting fluid are emulsifiers, surfactants, corrosion inhibitors and biocides.

After a long use, cutting fluid loses its lubricating property and generate a toxic waste. It contains heavy metals, biocides, microorganisms and harmful decomposition products. It is hard to use biological method to treat the cutting fluid due to its toxicity. Conventional treatment methods of oil-water emulsions are skimming, gravity setting, emulsion breaking,[1] chemical de-emulsification,[2] flotation,[3] combination of destabilization and flotation,[4] and membrane.[5,6] Some researchers introduce supercritical water oxidation[7] to treat cutting fluid but this method consumes a lot of energy.

Adsorption is a promising emerging technology to remove oil from oil-in-water emulsion. Adsorbents used are peat,[8] mixture of Ca and Mg oxides,[9] activated carbon, etc. One of the interesting natural absorbent is chitosan due to its excellent properties, such as biodegradability, hydrophilicity, biocompability, adsorption property, flocculating ability, polyelectrolisity and antibacterial property. Amino ($-NH_2$) group at C-2 and two hydroxyl (-OH) groups at C-3 and C-6 on chain of chitosan serve as coordination and reaction

*Corresponding Author. E-mail: sangobtip@gmail.com

sites.[10] Previous works used chitosan to adsorb heavy metals,[11-15] reactive dyes,[16,17] and residual palm-oil.[18,19] In view of the fact that, no work has been done in the literature regarding to adsorb cutting fluid on chitosan or SDS-modified chitosan. Furthermore, not many studies have been done with real effluent.

Therefore, the purpose of this work is to investigate an adsorption of cutting fluid on to chitosan and modified chitosan with sodium lauryl sulphate (called SDS-modified chitosan). This study can be listed as a novel work. Series of batch adsorption experiments were conducted to determine a performance of chitosan and SDS-modified chitosan as adsorbent for cutting fluid. Several of the physicochemical parameters of the adsorption (i.e. initial concentration of cutting fluid, contact time, pH of the fluid) were evaluated at the dynamic and equilibrium conditions. The isotherm and kinetic models were determined to explain the experimental data. Moreover, this work also presents an adsorption performance of chitosan and SDS-modified chitosan to treat the synthetic cutting fluid and cutting fluid effluent. This information will be useful for further application in treatment of practical cutting fluid wastewater.

Experimental

Materials. Chitosan flake (95% degree of deacetylation; average molecular weight: 700,000; extract from shrimp shell) was purchased from The Sea Fresh Co., Ltd., Thailand. Sodium hydroxide (NaOH) was purchased from Lab Scan. Acetic acid was purchased from Carlo Erba. Sodium lauryl sulphate was purchased from Ajax Finechem Co., Ltd., Australia. All the reagents used were reagent grade. Deionized water was used to prepare all solutions.

Preparation of Chitosan Beads and Modified Chitosan Fibers. 2.0 g of chitosan flake was dissolved in 100 cm^3 of 2 % v/v aqueous acetic acid solution. The chitosan solution was stirred by motor stirrer (IKA Labortechnik model RW 20.n, Malaysia) at 300 rpm for 24 h and at room temperature. The solution was then pumped by a peristaltic pump (Master Flex, Easy-Load II; model 77200-60, tubing L/S^{TM}14, U.S.A) and dropped through a needle (Ø1.2 mm.) into 1,000 cm^3 of 1 M NaOH solution. Hydrogel beads were then formed and left in the solution for 12 h to obtain hardened beads, as shown in Figure 1(a). The beads were then washed by deionized water for several times and stored in deionized water.

SDS-modified chitosan fibers were prepared by injecting 20 cm^3 of 20 cmc sodium lauryl sulphate (SDS) to 100 cm^3 of chitosan solution. The mixture was stirred by motor stirrer for 10 min at 150 rpm and at room temperature. Fibers were formed and then washed by deionized water for several times to eliminate the excess of sodium lauryl sulphate and acetic acid.[20] SDS-modified chitosan fibers, as shown in Figure 1(b), were stored in deionized water.

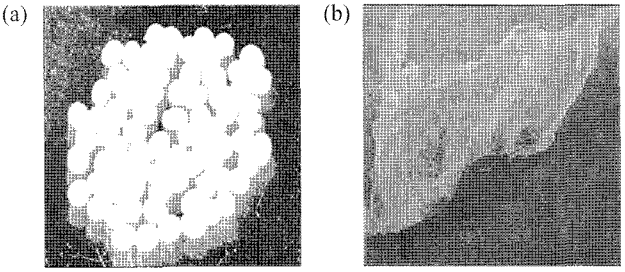

Figure 1. Adsorbent used in this study: (a) chitosan and (b) SDS-modified chitosan.

Measurement of Hydrophobic Property and Specific Surface Area (BET) of Adsorbents. Hydrohobic property of chitosan and SDS-modified chitosan were investigated by hydrophobic index and contact angle measurement. For hydrophobic index, 1.0 g of adsorbent was soaked in cutting fluid or deionized water until equilibrium had been reached. The adsorption capacity was calculated as {(weight of the adsorbed adsorbate/weight of the adsorbent) × 100}. Hydrophobic index was then computed as adsorption capacity of cutting fluid/adsorption capacity of deionized water.

A Glass plate was cleaned by acetone and then immersed into chitosan solution. The solution attaching on the surface of the glass plate was coagulated by 1 M NaOH. The hydrogel was then formed on the surface and washed by deionized water for several times. In case of SDS-modified chitosan, it was attached on the surface of the clean glass plate prior to measure the contact angle. The hydrophobic property of the adsorbents was investigated via contact angle measurement using the FTA 200 (Germany). The SCA 20 for OCA 15 plus and PCA was used to interpret the data. Contact angles were measured by sessile drop technique. Reported contact angles were the average of seven measurements which carried out on different location of surface of the adsorbents. A cutting fluid droplet was placed on the surface through a micro-syringe, and the contact angle was monitored under a microscope with sufficient enlargement and scanned by a video camera. Its signal was processed by a computer and the contact angles were evaluated by the Image Tool program.

The Brunauer-Emmet-Teller (BET) method (Quantachrome Corporation Autosorb) was used to determine the surface area and size of pore diameter of the prepared adsorbents by N_2 adsorption at -196 °C. Prior to N_2 adsorption, the samples were degassed at 120 °C for 6 h with Belprep flow (Japan). The surface area and size of pore diameter of each adsorbent were analyzed by Autosorb ANAGAS Software Version 2.10.

Zeta Potential Measurement. A Malvern Zetasizer (Model 3000 HAS, Malvern corp, U.K.) was used to determine a magnitude of zeta potential of the adsorbents. 0.2 g of each dried adsorbent was powered and then stirred in 200 cm^3 of deionized water by a motor stirrer at 350 rpm for 24

h to obtain dispersion. The supernatant was taken to measure zeta potential. To measure zeta potential of synthetic cutting fluid, 0.01 g of cutting fluid was suspended in 200 cm^3 of deionized water. The emulsion was stirred by motor stirrer at 1,200 rpm and at room temperature for 10 min. After that the emulsion was left for 30 min. The pH of dispersion and synthetic cutting fluid were adjusted with 0.1 M HCl or 0.1 M NaOH aqueous solution. The reported values for zeta-potential represent the mean value of five measurements.

Adsorption Experimental. Synthetic cutting fluid was prepared by stirring a desired amount of commercial cutting fluid (1.0–30.0 g) in 1,000 cm^3 of deionized water for 10 min to obtain the fluid at desired initial concentration. 1.0 g of adsorbents were weighted and added into the flask which contained 50 cm^3 of the synthetic cutting fluid. The mixture was shaken by an orbital shaker (PNP model OS 3) at 120 rpm and at room temperature. pH of the synthetic cutting fluid was varied from 3 to 11 by 0.1 M HCl and 0.1 M NaOH. At time interval, the fluid was taken to determine the residual concentration of the cutting fluid. The initial and residual concentration of cutting fluid were analyzed by a visible spectrophotometer (WTW, model Photo Lab Spektral, Germany) at wavelength 395 nm. To investigate an adsorption of effluent on the adsorbents, the cutting fluid effluent from Department of Mechanic Engineering, Faculty of Engineering, Chulalongkorn University was used. The adsorption capacity was calculated according to:

$$q_e = \frac{(C_0 - C_e)V}{m} \quad (1)$$

where q_e is the adsorption capacity (g/kg), C_0 is the initial concentration of cutting fluid (g/m^3), C_e is the equilibrium concentration of cutting fluid (g/m^3), V is the volume of the fluid (m^3) and m is the weight of adsorbent (kg).

Fourier Transform Infra-red Spectroscopy (FT-IR). Functional groups of fresh adsorbents and used adsorbents were analyzed by FT-IR spectra. The dried of fresh and used adsorbents were powdered and mixed with postassium bromide (KBr) and then pressed into pellet under pressure. Infrared spectra were measured with a Pekin-Elmer Model 2000 (USA) at 20 °C. The spectrum of an empty cell was used as the background. IR spectra in the range 4000-400 cm^{-1} were scanned in spectrum. An average of 10 scans was made for each sample at a resolution of 4 cm^{-1}.

Heat of Combustion. The Parr model 1341 oxygen bomb calorimeter, Parr instrument company (USA) was used to determined heat of combustion of adsorbent before and after adsorption. The amount of heat of combustion was calculated according to:

$$H_g = \frac{TW - e_1 - e_2 - e_3}{M} \quad (2)$$

where H_g is the gross heat of combustion (J/g), T is net corrected temperature rise (K), W is energy equivalent of calorimeter (J/K), e_1 is correction in calories for heat of formation of nitric acid (J), e_2 is correction in calories for heat of formation of sulfuric acid (J), e_3 is correction in calories for heat of formation of fuse wire (J) and M is weight of sample (g).

Scanning Electron Microscope (SEM). Scanning electron microscope image (SEM, JEOL, Model JSM-5410 LV, Japan) was used to obtain information about the morphology of adsorbents before and after adsorption.

Results and Discussion

Hydrophobic Property and Specific Surface Area (BET). Hydrophobic property of chitosan and SDS-modified chitosan was determined by hydrophobic index and contact angle, as shown in Table I. The value of hydrophobic index for chitosan is less than that of SDS-modified chitosan. This indicates that SDS-modified chitosan is more hydrophobic than chitosan. From the magnitudes of contact angle of cutting fluid on the surface of chitosan and SDS-modified chitosan, contact angle of chitosan is greater than SDS-modified chitosan. Less in contact angle implies to the less in hydrophilic property. Additionally, the hydrophobicity of the chitosan can be tuned by synthesis parameters, such as by modification with sodium lauryl sulphate. This also confirms that hydrophobic index result. Considering the specific surface area and size of pore diameter of chitosan and SDS-modified chitosan, it is also found from Table I that chitosan has more surface area than SDS-modified chitosan around 9.1 times and has larger pore diameter around 1.1 times.

Zeta Potential Measurement. Zeta potentials of chitosan and SDS-modified chitosan as a function of solution pH

Table I. Contact Angle, Hydrophobic Index, Surface Area and Pore Diameter Size of Chitosan and SDS-Modified Chitosan

	Chitosan	SDS-Modified Chitosan
Contact angle (degree)	24.7	18.5
Hydrophobic index	1.44	6.03
Surface area (m^2/g)	6.12	0.67
Pore diameter (nm)	1.67	1.49

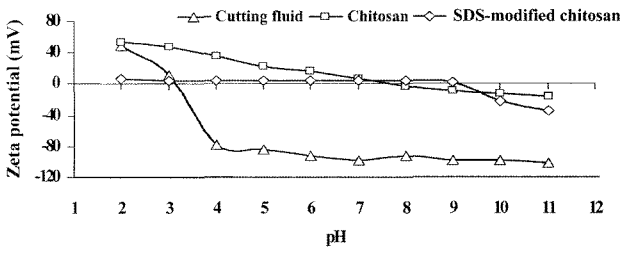

Figure 2. Variation of solution pH on zeta potential of synthetic cutting fluid, chitosan and SDS-modified chitosan.

values are shown in Figure 2. Zeta potentials of chitosan are positive in an acidic solution but negative in a basic condition. The point of zero charge (PZC) of chitosan is obtained at pH 7.8 which is close to the pKa value of 6.4-6.7 for the amino group in chitosan reported by others.[21] Below pH 7.8, the magnitude of zeta potentials of the chitosan increased with the decrease of solution pH values from 7.8 to 2. This can be attributed to the protonation of the amino groups in the chitosan (i.e., from $-NH_2$ to $-NH_3^+$). From pH 7.8 to 11, the negative zeta potentials of the chitosan are found. This indicates that the amino groups in the structure of chitosan are not deprotonated under these basic conditions (i.e., from $-NH_2$ to $-NH^-$).

From Figure 2, PZC of SDS-modified chitosan is obtained at pH 9. The magnitude of zeta potentials of SDS-modified chitosan is around +5 mV in a range of pH from 2 to 9. This can be said that SDS-modified chitosan is not protonated by hydrogen ions in this range of pH. From pH 9 to 11, magnitude of zeta potentials of the modified chitosan becomes negative about –40 mV at pH 11. The negative charges of SDS-modified chitosan may be due to dissociation of H^+ from the primary group of C-6 in the modified chitosan.

The repulsive force dominates the dispersion force between the emulsion droplets, where zeta potential shifts to negative values.[22] The zeta potentials of the synthetic cutting fluid at various pH conditions are also included in Figure 2. The synthetic cutting fluid has negative surface charges when pH is above 3.2 but has positive surface charges when pH is below 3.2. PZC of synthetic cutting fluid is obtained at pH 3.2 which is close to the pKa value of 3 for the carboxylic group in fatty acid. When the magnitude of zeta potential is in a range of +20 mV to -20 mV, the attractive force is a domain.[23] From Figure 2, the synthetic cutting fluid is a stable oil-in-water emulsion at pH > 4. The coagulation of emulsion does not occur.

Contact Time and Initial Concentration of Cutting Fluid Studies. The adsorption capacity of synthetic cutting fluid on chitosan and SDS-modified chitosan as a function of

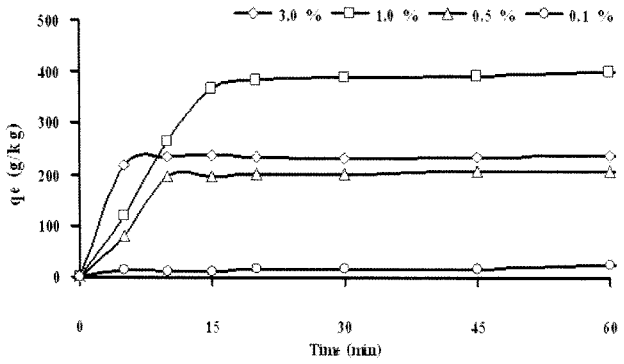

Figure 3. Adsorption capacity of synthetic cutting fluid on chitosan as a function of contact time when varying initial concentration of synthetic cutting fluid from 0.1 to 3.0% wt/v at pH 3.

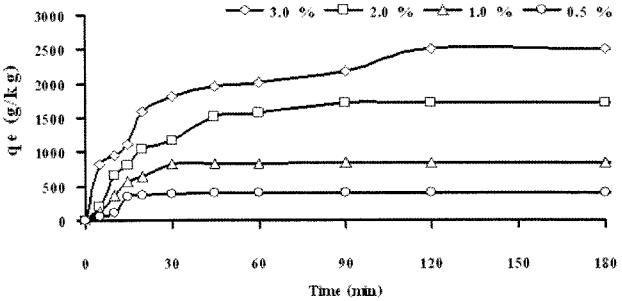

Figure 4. Adsorption capacity of synthetic cutting fluid on SDS-modified chitosan as a function of contact time when varying initial concentration of synthetic cutting fluid from 0.5 to 3.0% wt/v at pH 3.

contact time and initial concentration of synthetic cutting fluid at pH 3 are presented in Figure 3 and Figure 4, respectively. When holding an initial concentration of synthetic cutting fluid, the adsorption capacity on chitosan increases within the first 15 min of contact time. There is no change in the adsorption capacity when the contact time is longer. This implies that the equilibrium adsorption is obtained after 15 min. While the adsorption capacity on SDS-modified chitosan increases significantly within the first 60 min of contact time. The equilibrium adsorption of SDS-modified chitosan is obtained when the contact time is longer than 120 min.

An increase in initial synthetic cutting fluid concentration from 0.1 to 1.0% wt/v leads to an increase in the adsorption capacity of cutting fluid on chitosan. Further increasing in initial synthetic cutting fluid concentration from 1.0 to 3.0% wt/v, the adsorption capacity of synthetic cutting fluid on chitosan is decreased significantly. Considering the adsorption capacity of synthetic cutting fluid on SDS-modified chitosan, it can be seen from Figure 4 that the adsorption capacity increases from 450 to 2,500 g/kg when the initial synthetic cutting fluid concentration increases from 0.5 to 3.0% wt/v. Additionally, when increasing in the initial concentration of the fluid, longer contact time is needed to reach its equilibrium adsorption. From Figures 3 and 4, it can be noted that the adsorption capacity of synthetic cutting fluid on SDS-modified chitosan is greater than that on chitosan dramatically due to render hydrophobic of SDS-modified chitosan. This was confirmed by contact angle results.

pH of Emulsion. Since the zeta potentials of synthetic cutting fluid, chitosan and SDS-modified chitosan are all pH-dependent, series of batch adsorption experiments were conducted at various initial pH values. It is necessary to investigate the effect of pH on adsorption capacity, because pH affects not only the surface charges of the adsorbents and the cutting fluid droplets but also the degree of adsorption of cutting fluid during the reaction. Additionally, emulsion breaking is normally brought about changing the pH

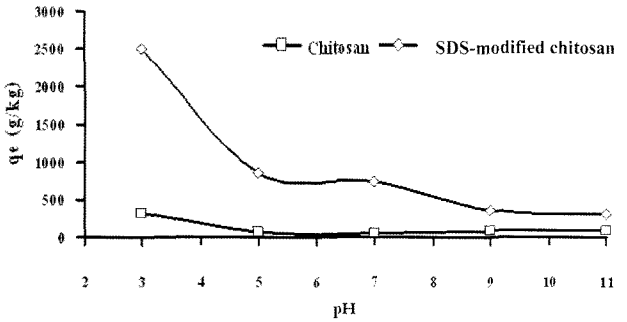

Figure 5. Adsorption capacity of synthetic cutting fluid on chitosan and SDS-modified chitosan at various pH conditions.

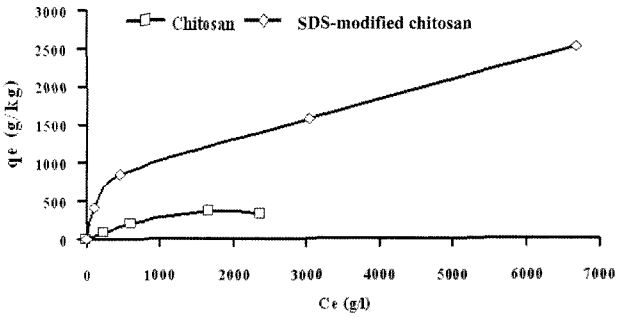

Figure 6. Equilibrium adsorption of synthetic cutting fluid on chitosan and SDS-modified chitosan.

value or adding of inorganic coagulants.[22] To examine the effect of pH on the adsorption capacity, the pH of synthetic cutting fluid was varied from 3 to 11. Figure 5 shows the effect of pH on capacity of chitosan and SDS-modified chitosan on synthetic cutting fluid adsorption. The capacities of the chitosan and SDS-modified chitosan are indeed dependent on the pH of emulsion. The capacities of both adsorbents decrease continuously when the initial pH of emulsion is increased from 3 to 11. SDS-modified chitosan gives greater adsorption capacities than chitosan for a whole range of pH. A significant change in the adsorption capacity of the adsorbents occurs between pH 3 and 5.

As described above, adsorption of synthetic cutting fluid on chitosan and SDS-modified chitosan involves the protonation of amino groups in chitosan and in SDS-modified chitosan. Therefore, the adsorption capacity can be expected to increase if the amount of protonated amino groups increases. A high concentration of H^+ at a low pH leads to an increased number of protonated amino sites. On the other hand, the increase of pH of emulsion reduces the concentration of H^+. As a result, the adsorption capacity decreases with increasing pH value.

Additional, electrostatic interactions between synthetic cutting fluid and adsorbent surface affect the adsorption performance. PZC of synthetic cutting fluid is around 3.2 (see Figure 2). Destabilization of emulsion is obtained when decreasing pH value. This leads to encourage the adsorption capacity.[18] In a range of pH used in this study, magnitude of zeta potentials of chitosan is higher than SDS-modified chitosan. Therefore, adsorption capacity of chitosan is lower than SDS-modified chitosan, as shown in Figure 5. The acidic condition acts as a catalyst to enhance the adsorption of synthetic cutting fluid on the adsorbents. In basic condition, the adsorption capacity of synthetic cutting fluid on adsorbents is decreased due to deprotonation of adsorbents and electrostatic repulsive interactions.

Equilibrium Adsorption. Figure 6 shows equilibrium adsorption of synthetic cutting fluid on 1.0 g weight dosage of chitosan and SDS-modified chitosan at pH 3. Adsorption capacity of synthetic cutting fluid on both types of adsorbents is also compared. The synthetic cutting fluid adsorption on chitosan is affected via the coordination with the unprotonated amino groups of chitosan. The adsorption of synthetic cutting fluid on SDS-modified chitosan is affected via hydrophobic interaction of sodium lauryl sulphate and via amino groups of chitosan. It has been reported that surface area of adsorbents and size of pore diameter are a factor in adsorption,[24] but increasing in surface area and size of pore diameter of adsorbent can not encourage adsorption of cutting fluid. Even though chitosan has more surface area and larger pore diameter than SDS-modified chitosan, as shown in Table I, the adsorption capacity of chitosan is lower than SDS-modified chitosan (see Figure 6). This can be attributed that surface area and size of pore diameter of adsorbent are not a main factor in adsorption of cutting fluid. Figure 7 shows chemical structure of chitosan and SDS-modified chitosan. Sodium lauryl sulphate interacts with amino groups in chitosan to form aliphatic groups. Based on the hydrophobic index and contact angle results, SDS-modified chitosan render hydrophobic property than chitosan. Adsorption capacity of synthetic cutting fluid on SDS-modified chitosan is greater than that on chitosan. Therefore, not only surface area and size of pore diameter of adsorbent but also hydrophobic interaction between adsorbent and adsorbate should be considered as an important factor in adsorption. Methylene groups in SDS-modified chitosan have a higher binding affinity for the adsorption of synthetic cutting fluid. Chitosan binds the synthetic cutting fluid with its amino sites near the outer surface. Eventually when time goes by or when initial concentration of cutting

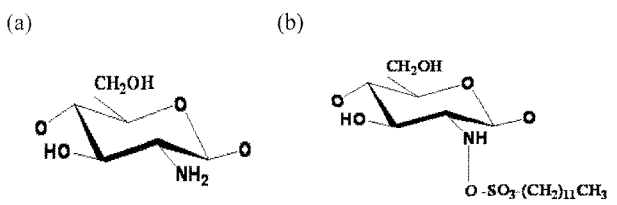

Figure 7. Structure of (a) chitosan and (b) SDS-modified chitosan.

Table II. Characteristics of Cutting Fluid Effluent from Turning Process

Parameters	Concentration
COD (g/m^3)	12,00
Oil and grease (g/m^3)	2342
Total dissolved solid (g/m^3)	853
Total suspended solid (g/m^3)	2339
Total solid (g/m^3)	3192
Fe^{3-} iron (% wt) *	55
pH 5.96	

*Determined by X-Ray Fluorescence Spectrometer (XRF).

fluid is increased from 1.0 to 3.0% wt/v, the adsorbed synthetic cutting fluid on chitosan starts to clog the pores near the outer surface so synthetic cutting fluid can no longer diffuse to the active sites deep within the interior surface.

Adsorption of Cutting Fluid Effluent. Table II presents characteristics of cutting fluid effluent from the turning process. COD of effluent is quite high due to a contamination of mineral oil and bacteria. The effluent contains about 2,342 g/m^3 of oil and grease. Total solid in the effluent is around 3,292 g/m^3. From X-Ray Fluorescence Spectrometer (XRF) results, it is found that there are 55 wt% of iron (Fe^{3-}) contained in the effluent. Figure 8 shows the adsorption capacity of cutting fluid effluent on 1.0 g weight of chitosan and of SDS-modified chitosan at pH 3. In the first 10 min of contact time, capacity of chitosan for cutting fluid effluent adsorption increases dramatically. Equilibrium adsorption of chitosan occurs within 10 min and the capacity of chitosan is around 720 g/kg. For SDS-modified chitosan, it takes around 90 min to reach its equilibrium. Adsorption capacity of cutting fluid effluent on SDS-modified chitosan is greater than chitosan slightly. It is quite interesting that difference in adsorption capacity of cutting fluid effluent on SDS-modified chitosan and on chitosan is less (see Figure 8). When adsorbing synthetic cutting fluid, the capacity between SDS-modified chitosan and chitosan

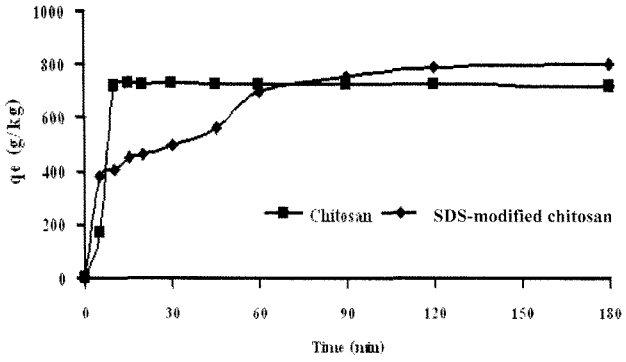

Figure 8. Adsorption capacity of cutting fluid effluent on chitosan and SDS-modified chitosan at pH 3.

is quite different (see Figures 3 and 4). This can be explained that Fe^{3+} ions contained in the effluent encourage the adsorption capacity of chitosan. To obtain more information about the effect Fe^{3+} on the adsorption capacity on chitosan and SDS-modified chitosan, the same amount of Fe^{3-} was added to 1% wt/v of synthetic cutting fluid. The experimental results reveal that equilibrium adsorption of synthetic cutting fluid on chitosan is increased to around 750 g/kg within the first 10 min of contact time when adding Fe^{3+}. The adsorption capacity of SDS-modified chitosan when adding Fe^{3+} is quite similar to the case of no adding Fe^{3+}. Considering magnitudes of zeta potential of chitosan and SDS-modified chitosan when adding 55 wt% of Fe^{3+} at pH 3, zeta potential of chitosan reduces to +32 mV while the zeta potential of SDS-modified chitosan does not changes much. As described earlier, it implies that hydrophobic interaction between chitosan and cutting fluid is encouraged when adding Fe^{3+} and then leads to achieve more adsorption capacity.

Adsorption Isotherm. Adsorption isotherm is important in describing how cutting fluid interrelate with chitosan and SDS-modified chitosan. Three well-known mathematical models (i.e. Langmuir, Freundlich and Brunauer Emmett and Teller (BET) isotherm) are used to analyze the adsorption isotherm results.

Langmuir equation is expressed as follows:

$$\frac{1}{x/m} = \frac{1}{B} + \frac{1}{ABC} \tag{3}$$

where x is the amount of cutting fluid adsorbed (kg), m is the weight of adsorbent (kg), C is the concentration of cutting fluid remaining in solution after adsorption (g/m^3), A and B are Langmuir constant.

Freundlich equation is expressed as follows:

$$\frac{x}{m} = KC^{1/n} \tag{4}$$

where x is the amount of cutting fluid adsorbed (kg), m is the weight of adsorbents (kg), C is the concentration of cutting fluid remaining in solution after adsorption (g/m^3), K and n are Freundlich constants.

BET equation is expressed as follows:

$$\frac{c}{(C_s - c)x/m} = \frac{1}{a(x_m)} + \frac{a-1}{ax_m} \tag{5}$$

where x_m is the amount of cutting fluid adsorbed corresponding to complete monolayer coverage (g/kg), C_s is the saturation concentration of cutting fluid (g/m^3), c is the concentration of cutting fluid at equilibrium stage (g/m^3) and a is the BET constant.

Parameters of Langmuir, Freundlich and BET isotherms are computed and shown in Table III. The Langmuir isotherm fits very well with data of adsorption capacity of synthetic cutting fluid and cutting fluid effluent on chitosan,

Table III. Adsorption Isotherms for Cutting Fluid Adsorption on Chitosan and SDS-Modified Chitosan

Cutting Fluid	Adsorbents	Langmuir				Freundlich			BET		
		A	B	R_L	R^2	K	n	R^2	a	X_m	R^2
Synthetic	Chitosan	0.0001	0.700	0.00030	0.965	-0.029	-	0.824	-1.16	-0.27	0.100
	SDS-Modified Chitosan	0.0270	1.339	0.00002	0.804	0.864	180.56	0.637	1.00	47.30	0.980
Effluent	Chitosan	0.0041	0.065	0.00002	0.887	-0.143	-	0.826	0.95	9.07	0.050
	SDS-Modified Chitosan	0.0002	0.765	0.00008	0.977	0.050	6.46	0.946	2.62	1.05	0.989

indicating that the synthetic cutting fluid and cutting fluid effluent are adsorbed on the surface of chitosan beads as monolayer. In case of adsorption capacity of chitosan, the separation factor (R_L) value is in a range of 0 to 1. This indicates a favorable adsorption of synthetic cutting fluid and cutting fluid effluent on chitosan. The Langmuir constant, B, in case of SDS-modified chitosan is greater than that in case of chitosan. This reveals that cutting fluid prefer to adsorb on SDS-modified chitosan. The Freundlich isotherm does not fit well with the chitosan and SDS-modified chitosan data. In case of SDS-modified chitosan as an adsorbent, the value of Freundlich constant, n, is high. This means that SDS-modified chitosan can adsorb cutting fluid even though the initial concentration of the fluid is increased. BET isotherm fits very well with SDS-modified chitosan data. The BET constant, a, obtained from SDS-modified chitosan data is greater than chitosan data. This indicates that energy interaction between cutting fluid and surface of SDS-modified chitosan is greater. From the isotherm results, it also confirms that adsorption capacity of cutting fluid on SDS-modified chitosan is greater than chitosan.

Adsorption Kinetics. In order to investigate the mechanism of adsorption, the pseudo first-order and the pseudo second-order adsorption models are used to test dynamic experimental data.

Pseudo first-order equation is expressed in the form of:

$$\frac{dq_t}{dt} = k_1(q_e - q_t) \tag{6}$$

where q_t is the amount of adsorption at time t (g/kg), k_1 is the rate constant of pseudo first-order adsorption (1/min). After integration and applying the initial condition $q_t = 0$ at $t = 0$, eq. (6) becomes

$$\log(q_e - q_t) = \log q_e - \frac{k_1}{2.303}t \tag{7}$$

The pseudo second-order equation is based on adsorption equilibrium capacity and expressed in the form of:

$$\frac{dq_t}{dt} = k_2(q_e - q_t)^2 \tag{8}$$

where k_2 is the rate constant of pseudo second-order adsorption (kg/g-min). Integrating eq. (8) and applying initial condition, it is

$$\frac{1}{(q_e - q_t)} = \frac{1}{q_e} + k_2 t \tag{9}$$

or equivalent to

$$\frac{t}{q_t} = \frac{1}{k_2 q_e^2} + \frac{1}{q_e}t \tag{10}$$

It is noted that k_2 and q_e can be calculated from the intercept and slope of plot of (t/q_t) vs. t and there is no need to know any parameter in advance. Normally pseudo first-order equation is expressed in range of reaction only and does not fit well with the whole range of contact time. It is generally applied over the initial stage of adsorption processes, although it has been effectively used to describe adsorption reaction.

Table IV shows the rate constant of pseudo first- and pseudo second-order adsorption. It is found that the correlation coefficient (R^2) for the pseudo first-order adsorption is far from unity. This suggests that the adsorption of synthetic cutting fluid and cutting fluid effluent on chitosan are not a pseudo first-order reaction. The correlation coefficient for the pseudo second-order reaction is almost to 1. This indicates that the adsorption of synthetic cutting fluid and cutting fluid effluent on SDS-modified chitosan agree very

Table IV. Kinetic Parameters for Cutting Fluid Adsorption on Chitosan and SDS-Modified Chitosan

Cutting Fluid	Adsorbents	Pseudo First-order		Pseudo Second-order	
		k_1	R^2	k_2	R^2
Synthetic	Chitosan	1.317	0.409	0.0021	0.999
	SDS-Modified Chitosan	3.251	0.906	0.0049	0.998
Effluent	Chitosan	0.084	0.630	0.0028	0.999
	SDS-Modified Chitosan	2.636	0.914	0.0144	0.998

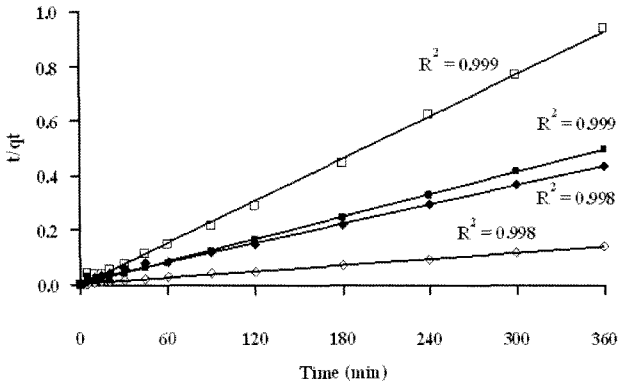

Figure 9. Plot of pseudo second-order kinetic model for synthetic cutting fluid adsorption on □ chitosan and ◊ SDS-modified chitosan; for cutting fluid effluent adsorption on ■ chitosan and ♦ SDS-modified chitosan.

well with the pseudo second-order kinetic model. The rate constants of both models, i.e. k_1 and k_2 proves that SDS-modified chitosan has a higher and enhanced adsorption rate compared to chitosan.

Figure 9 presents plot of pseudo second-order kinetic model for cutting fluid adsorption on chitosan and SDS-modified chitosan. The straight line in plot t/q_t vs. t fits very well with the experimental data. The pseudo second-order model is based on the adsorption capacity. It predicts the behavior over the whole range of studies supporting the validity and is in agreement with chemisorption being the rate-controlling.

Adsorption Mechanism. From the results of pseudo first- and second-order models, the present findings remain uncertain about the adsorption mechanism. The intraparticle diffusion model is integrated. This can be described as

$$q_t = k_i t^{0.5} \tag{11}$$

where k_i is an intraparticle diffusion rate constant (g/kg-min$^{0.5}$). The k_i is the slope of straight-line portions of plot q_t vs. $t^{0.5}$. The initial rates of intraparticle diffusion are obtained by linearization of the curve $q_t = f(t^{0.5})$.

Table V shows the rate parameter for chitosan and SDS-modified chitosan. Four rate parameters are found for SDS-modified chitosan but only two rate parameters are presented for chitosan. Therefore, the mechanism of cutting fluid adsorption on SDS-modifies chitosan involves in four steps while the adsorption on chitosan involves in only two steps. The first rate (k_{i1}) for chitosan and SDS-modified chitosan is higher compared to the others. This suggests that the first stage is the instantaneous adsorption stage. The second stage is the final equilibrium stage for adsorption on chitosan while it is the gradual adsorption for adsorption on SDS-modified chitosan. The third one is the diffusion to the internal pore of SDS-modified chitosan and the last one is the final equilibrium stage. For mechanism of cutting fluid adsorption on chitosan, it reveals that the adsorption mechanism on chitosan occurs at the external surface of chitosan. The cutting fluid is adsorbed on surface of chitosan. It does not move into the internal surface of chitosan. Therefore, the pore on the surface of chitosan can be clogged when increasing in the initial concentration and consequently reduce the adsorption capacity of chitosan. This also confirms the effect of initial cutting fluid concentration on adsorption capacity of chitosan. The mechanism adsorption of chitosan and SDS-modified chitosan are confirmed by the intraparticle diffusion model.

FT-IR Spectra. Figure 10 shows FT-IR spectra of synthetic cutting fluid and cutting fluid effluent. It is found that the main component of synthetic cutting fluid and effluent is mineral oil. The alkane appears at 2925 and 2855 cm^{-1}, methylene and methyl appears at 1465 and 1375 cm^{-1}. The long chain of methylene group, which has more than four carbon atoms, appears at 720 cm^{-1}. The emulsifier that may

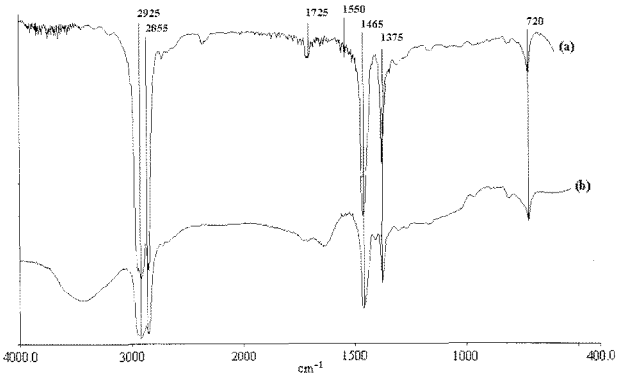

Figure 10. FT-IR spectra of (a) synthetic cutting fluid and (b) cutting fluid effluent.

Table V. Rate Parameters of Intraparticle Diffusion Model

Cutting Fluid	Adsorbents	Rate Parameter, k_i (i = 1-4)			
		k_{i1}	k_{i2}	k_{i3}	k_{i4}
Synthetic	Chitosan	152.99	0.15	-	-
	SDS-Modified Chitosan	291.05	164.72	152.99	0.62
Effluent	Chitosan	199.29	0.320	-	-
	SDS-Modified Chitosan	136.15	40.18	17.59	3.18

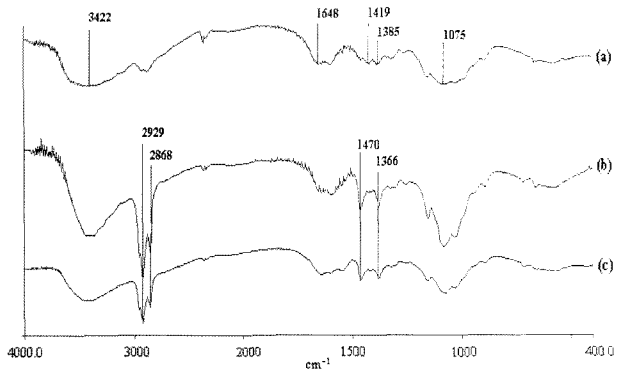

Figure 11. FT-IR spectra of chitosan (a) before adsorbing cutting fluid, (b) after adsorbing synthetic cutting fluid, and (c) after adsorbing cutting fluid effluent.

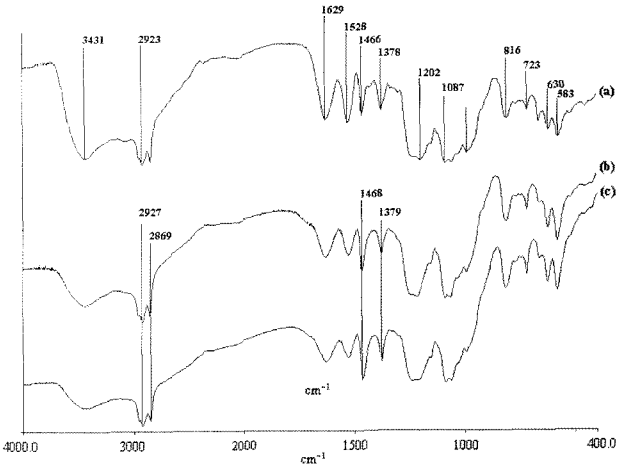

Figure 12. FT-IR spectra of SDS-modified chitosan (a) before adsorbing cutting fluid, (b) after adsorbing synthetic cutting fluid, and (c) after adsorbing cutting fluid effluent.

be naphthenic included aromatic appears at 1550 cm^{-1} and C=O appears at 1725 cm^{-1}.[25] The FT-IR spectra of cutting fluid effluent is similar to the synthetic cutting fluid. The broad peaks at 3600-3000 cm^{-1} in the FT-IR spectra of cutting fluid effluent mean H-bonded of water in effluent.

The spectra of fresh chitosan and chitosan after adsorption are shown in Figure 11. The spectra of fresh chitosan appears O-H stretching at 3422 and 1419 cm^{-1}, N-H bending at 1648 cm^{-1}, C-O stretching at 1385 cm^{-1} and C-O stretching at 1075 cm^{-1}. Chitosan after adsorption, there are sharp peaks of alkane appeared at 2929 and 2868 cm^{-1}, methylene at 1470 cm^{-1} and methyl at 1366 cm^{-1}. This confirms that chitosan can adsorb synthetic cutting fluid and cutting fluid effluent.

The spectra of SDS-modified chitosan before and after adsorption are presented in Figure 12. From Figure 12(a), the spectra of SDS-modified chitosan before adsorption appears O-H stretching at 3431 cm^{-1}, alkane at 2923 cm^{-1}, two peaks of N-H bending at 1629 and 1528 cm^{-1}, CH_2 at 1466 cm^{-1}, CH_3 at 1378 cm^{-1}, S=O at 1202 cm^{-1}, R-O-S three peaks at 1087, 1000 and 816 cm^{-1}, CH_2 long chain (more than four atoms) at 723 cm^{-1}, S-O at 630 cm^{-1} and =C-H at 583 cm^{-1}. This implies a chemical structure of SDS-modified chitosan, as shown in Figure 7(b). This is also supported by NMR result. It shows the quantify substitute ratio of chitosan and sodium lauryl sulphate is 1 to 1.5. Figures 12(b) and (c) show the spectra of SDS-modified chitosan after adsorption synthetic cutting fluid and cutting fluid effluent. It can be found that alkane appears at 2927 and 2869 cm^{-1}, at 1,468 cm^{-1} for methylene and at 1379 cm^{-1} for methyl. The appearance of alkane, methylene and methyl groups on modified chitosan demonstrates the adsorption of synthetic cutting fluid and cutting fluid effluent on SDS-modified chitosan.

Surface Morphology Observation by SEM. The surface morphology of chitosan before and after adsorption are shown in Figure 13. As can be seen in Figure 13(a), chitosan shows bumpy and fold of layers which are arranged homogenously. From Figures 13(b) and 13(c) that muddy-like substance is found after adsorbing the cutting fluid. The surface of chitosan is spread and covered with muddy-like or rough surface with bubble-like texture due to cutting fluid molecules which covered the chitosan. The chitosan after adsorbing the effluent has a lot of holes scattered on the surface. This may due to a degradation of the effluent.

Figure 14 presents SEM images of SDS-modified chito-

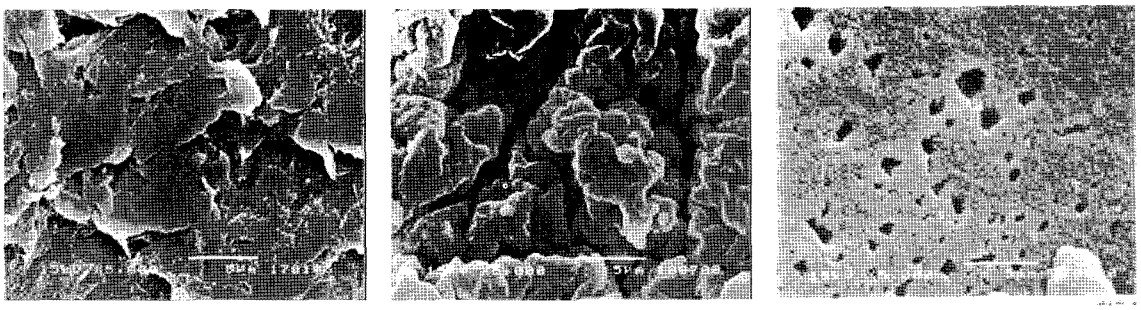

(a) (b) (c)

Figure 13. SEM micrographs of surface morphology of chitosan (a) before adsorbing cutting fluid, (b) after adsorbing synthetic cutting fluid, and (c) after adsorbing cutting fluid effluent.

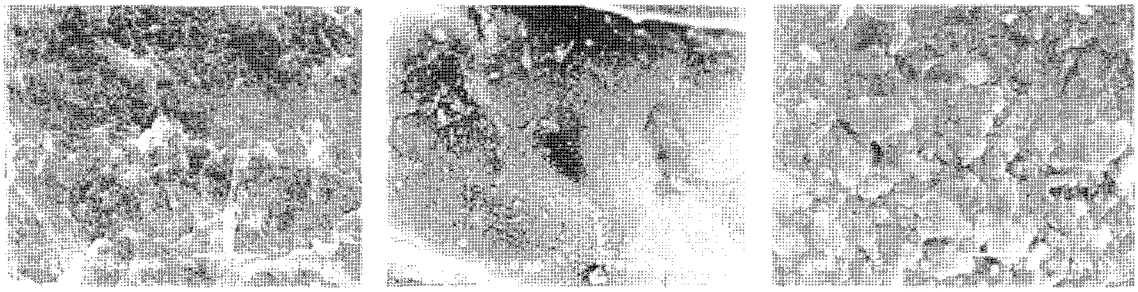

(a) (b) (c)

Figure 14. SEM micrographs of surface morphology of SDS-modified chitosan (a) before adsorbing cutting fluid, (b) after adsorbing synthetic cutting fluid, and (c) after adsorbing cutting fluid effluent.

Table VI. Heat of Combustion of Chitosan and SDS-Modified Chitosan before and after Adsorbing Cutting Fluid

Heat of Combustion (kJ/g)	Chitosan	SDS-Modified Chitosan
Before adsorbing cutting fluid	25.5	27.3
After adsorbing synthetic cutting fluid	38.6	52.6
After adsorbing cutting fluid effluent	51.9	57.3

san before and after adsorption. SDS-modified chitosan before adsorption has a patchy wave type distribution, as shown in Figure 14(a). From Figures 14(b) and 14(c), they reveal a muddy-like substance of SDS-modified chitosan after adsorbing cutting fluid. This also confirms that synthetic cutting fluid and cutting fluid effluent are adsorbed on SDS-modified chitosan.

Heat of Combustion. Heat of combustion of chitosan and SDS-modified chitosan before and after adsorption is determined, as shown in Table VI. It is observed that heating value of chitosan and SDS-modified chitosan after adsorption is higher. This may be a good motivation to use chitosan and SDS-modified chitosan, which adsorbed cutting fluid, as a solid fuel in order to get energy in return.

Conclusions

This study investigates an adsorption capacity of synthetic cutting fluid and cutting fluid effluent on chitosan and SDS-modified chitosan. As a conclusion, the adsorption capacity is affected significantly by the initial concentration of cutting fluid and pH. Adsorption capacity of SDS-modified chitosan increases with the initial concentration of cutting fluid from 0.5 to 3.0% wt/v at pH 3. The capacity of chitosan increases when increasing in initial concentration of cutting fluid from 0.1 to 1.0% wt/v at pH 3. Further increasing in the initial concentration of cutting fluid to 3.0% wt/v at pH 3, the adsorption capacity of chitosan is then decreased since the cutting fluid start to clog the pore near the outer surface. The capacities of chitosan and SDS-modified chitosan depend on pH. The capacities increase with decrease in pH. From the experimental results, it can be said that not only surface area and size of pore diameter of adsorbent but also hydrophobic interaction between adsorbent and adsorbate should be considered as an important factor in adsorption. From the adsorption isotherm models, Langmuir model fits well with experimental data of chitosan. BET model fits well with the adsorption data of SDS-modified chitosan. The pseudo first- and second-order kinetic models and intraparticle diffusion model are applied to explain the kinetic data. The adsorption kinetic model of cutting fluid on chitosan and SDS-modified chitosan is the pseudo second-order. The mechanism of cutting fluid adsorption on SDS-modifies chitosan involves in four steps: (1) diffusion of cutting fluid to the boundary surface of adsorbent; (2) diffusion through a liquid film at the surface to pores of adsorbent; (3) diffusion into the pores; (4) adsorption on the internal surface of adsorbent. For mechanism of cutting fluid adsorption on chitosan, it has only the first two steps: step 1 and step 2. These mechanisms are confirmed by the intraparticle diffusion model. FT-IR spectra, SEM micrographs and heat of combustion are used to prove the adsorption performance of cutting fluid on chitosan and SDS-modified chitosan.

Achnowledgements. This project was supported by the Thailand Research Fund (TRF) under Grant Number RSA5080012. Their support is gratefully acknowledged. The authors would like to thank Department of Mechanic Engineering, Faculty of Engineering, Chulalongkorn University for providing the cutting fluid effluent.

Nomenclature

a : BET constant
A : Langmuir constant
B : Langmuir constant
c : concentration of cutting fluid at equilibrium stage [g/m^3]
C : concentration of cutting fluid remaining in solution after adsorption [g/m^3]

C_e : equilibrium concentration of cutting fluid [g/m^3]
C_o : initial cutting fluid concentration [g/m^3]
C_s : saturation concentration of cutting fluid [g/m^3]
e_1 : correction in calories for heat of formation of nitric acid [J]
e_2 : correction in calories for heat of formation of sulfuric acid [J]
e_3 : correction in calories for heat of formation of fuse wire [J]
H_g : gross heat of combustion [J/g]
K : Freundlich constant
k_1 : rate constant of pseudo first-order adsorption [1/min]
k_2 : rate constant of pseudo second-order adsorption [kg/g-min]
k_i : intraparticle diffusion rate constant (g/kg-min$^{0.5}$)
m : weight of adsorbent [kg]
M : weight of sample [g]
n : Freundlich constant
q_e : adsorption capacity [g/kg]
q_t : amount of adsorption at time t [g/kg]
R^2 : correlative coefficient
R_L : separation factor
t : time [minute]
T : net corrected temperature rise [K]
V : volume of cutting fluid [m^3]
W : energy equivalent of calorimeter [J/K]
x : amount of cutting fluid adsorbed [kg]
x_m : amount of cutting fluid adsorbed corresponding to complete monolayer coverage [g/kg]

References

(1) J. Marchese, N. A. Ochoa, C. Pagliero, and C. Almandoz, *Environ. Sci. Technol.*, **34**, 2990 (2000).
(2) G. Ríos, C. Pazos, and J. Coca, *Colloid Surface A*, **138**, 383 (1998).
(3) A. Y. Hosny, *Sep. Technol.*, **6**, 9 (1996).
(4) N. Moulai Mostefa and M. Tir, *Desalination*, **161**, 115 (2004).
(5) M. Belkacem, H. Matamoros, C. Cabassud, Y. Aurelle, and J. Cotteret, *J. Membrane Sci.*, **106**, 195 (1995).
(6) P. Janknecht, A. D. Lopes, and A. M. Mendes, *Environ. Sci. Technol.*, **38**, 4878 (2004).
(7) J. R. Portela, J. López, E. Nebot, and E. Martínez de la Ossa, *J. Hazard. Mater.*, **88**, 95 (2001).
(8) T. Viraraghavan and G. N. Mathavan, *Oil Chem. Pollut.*, **4**, 261 (1988).
(9) C. Solisio, A. Lodi, A. Converti, and M. D. Borghi, *Water Res.*, **36**, 899 (2002).
(10) B. C. Son, K. Park, S. H. Song, and Y. J. Yoo, *Korean J. Chem. Eng.*, **21**, 1168 (2004).
(11) S. E. Bailey, T. J. Olin, R. M. Bricka, and D. D. Adrian, *Water Res.*, **33**, 2469 (1999).
(12) V. M. Boddu, K. Abburi, J. L. Talbott, and E. D. Smith, *Environ. Sci. Technol.*, **37**, 4449 (2003).
(13) J. R. Evans, W. G. Davids, J. D. MacRae, and A. Amirbahman, *Water Res.*, **36**, 3219 (2002).
(14) C. Jeon and W. H. Hll, *Water Res.*, **37**, 4770 (2003).
(15) W. S. Wan Ngah, C. S. Endud, and R. Mayanar, *React. Funct. Polym.*, **50**, 181 (2002).
(16) A. R. Cestari, E. F. S. Vieira, A. G. P. dos Santos, J. A. Mota, and V. P. de Almeida, *J. Colloid Interf. Sci.*, **280**, 380 (2004).
(17) M.-S. Chiou, P.-Y. Ho, and H.-Y. Li, *Dyes and Pigments*, **60**, 69 (2004).
(18) A. L. Ahmad, S. Sumathi, and B. H. Hameed, *Water Res.*, **39** 2483 (2005).
(19) A. L. Ahmad, S. Sumathi, and B. H. Hameed, *Chem. Eng. J.*, **108** 179 (2005).
(20) S. Pongstabodee, K. Piyamongkala, and L. Mekasut, Thai Patent No.0601004582.
(21) X. Zhang and R. Bai, *J. Colloid Interf. Sci.*, **264**, 30 (2003).
(22) A. I. Zouboulis and A. Avranas, *Colloid Surface A*, **172**, 153 (2000).
(23) J. M. Montgomery, *Water Treatment Principles and Design*, John Wiley and Sons, Inc., New York, 1985.
(24) L. D. Benefield, J. F. Judkins, and B. L. Weand, *Processes Chemistry for Water and Wastewater Treatment*, Prentice-Hall, Inc., Englewood, 1982.
(25) D. L. Pavia, G. M. Lampman, and G. S. Kriz, *Introduction to Spectroscopy*, 3^{ed}, Harcourt College Publishers, Orlando, 2001.